Title

Characterization and Catalytic Performance of Modified Nano-scale ZSM-5 for Acetone-to-Olefins Reaction

Author

Hiroki Konno, Teruoki Tago*, Yuta Nakasaka, Gaku Watanabe, Takao Masuda

Division of Chemical Process Engineering, Faculty of Engineering,

Hokkaido University, N13 W8, Kita-ku, Sapporo, Hokkaido 060-8628, Japan

** corresponding author should be addressed*

e-mail: tago@eng.hokudai.ac.jp

tel:+81-117066551

fax: +81-117066552

Research highlights

Characterization and Catalytic Performance of

Modified Nano-scale ZSM-5 for Acetone-to-Olefins Reaction

Hiroki Konno, Teruoki Tago*, Yuta Nakasaka, Gaku Watanabe, Takao Masuda

- Acidity modification of ZSM-5 zeolite was examined.
- Phenyl silane and Tri-phenyl silane were newly used as deactivators.
- Catalytic properties of ZSM-5 zeolites can be controlled.
- Modified ZSM-5 was effective in acetone-to-olefins reaction.

Abstract

In acetone to olefins (ATO) reaction using ZSM-5 zeolite, isobutylene is initially produced from decomposition of an acetone dimer, followed by dimerization of isobutylene and its cracking to form ethylene and propylene formation. Nano-scale ZSM-5 zeolite exhibited a stable activity in ATO reaction as compared with macro-scale ZSM-5. In order to improve the catalytic stability of the nano-scale ZSM-5, acidity control in the nano-scale ZSM-5 zeolite by SiO_2 unit formation was examined. Phenyl silane and tri-phenyl silane were newly used as deactivators. This modification allows the increase in the olefins yield as well as improvement of catalyst lifetime. In particular, the regioselective deactivation of acid sites located on the external surface of zeolite inhibits the aromatics formation. Moreover, the acidity control within the pore extremely improves the catalyst lifetime. The acidity-controlled nano-scale ZSM-5 zeolite exhibited stable olefins yield above 55 C-mol% for 180h.

Keywords

Acidity modification; Nano-zeolite; ZSM-5; Acetone conversion; Light olefins

1. Introduction

Light olefins are important basic raw materials for petrochemical industry and their demands are increasing every year [1-3]. Ethylene, propylene and isobutylene are the key building block for the production of chemical products, such as polyethylene (LDPE, HDPE), polypropylene (PP), polyvinyl chloride (PVC), polyacrylonitrile (PAN), ethylene oxide, propylene oxide, methyl methacrylate (MMA), ethyl tertiary-butyl ether (ETBE) and so on. These light olefins have been mainly produced by steam cracking of naphtha. However, because this process consumes more than 30% of the total amount of energy required in petrochemical refinement, the new efficient processes for light olefins production have been required. Promising candidate processes for light olefins production are naphtha catalytic cracking (NCC) [4-11], methanol-to-olefins (MTO) [12-14], ethanol-to-olefins (ETO) [15-17] and propane dehydrogenation (PDH) [18, 19].

Because a large amount of acetone is obtained as a by-product in the cumene process [20], we suggested light olefins synthesis from acetone (acetone-to-olefins, ATO) over zeolite catalyst, and reported that high light olefins yield was achieved using ZSM-5 zeolite [21] and alkali metal ion-exchanged Beta zeolite [22]. In this reaction, isobutylene was first produced from acetone via the formation of acetone dimer (diacetone alcohol) and trimer (iso-phorone), followed by production of propylene, ethylene and aromatics [21-27]. These are intermediates

in the series of reactions with coke as terminal products.

In our previous study, it is reported that the ZSM-5 zeolite was effective for suppression of aromatics formation. This is because the consecutive reaction mainly routed not via iso-phorone formation/decomposition as aromatics precursor but via diacetone alcohol formation/decomposition due to spatial limitation of ZSM-5 zeolite with 10-membered ring [21]. However, the non-desirable excessive reactions producing aromatics and coke due to light olefins consumption easily occur on acid sites around cross sectional space along with that near the external surface of zeolite crystal. Therefore, a method is desired for regioselective deactivation and acidity control of the acid sites of the zeolite crystals to prevent these non-desirable excessive reactions.

We have developed a method for the acidity modification of the acid sites of zeolite using organic silane compounds (Catalytic Cracking of Silane, denoted as CCS method) [28-30]. In the CCS method, a SiO_2 unit is formed on the acid sites where silane compound is chemically adsorbed. Accordingly, the acidity of the zeolite can be modified due to the SiO_2 formation on acid sites. Since the molecular diameter of the silane compounds depends on the types of organic groups bonding to Si atom, it is expected that the deactivation of the acid sites located on the external surface of the zeolite crystals can be achieved by utilizing the molecular sieving effect of the zeolites. Moreover, when silane compounds that are comparable or small in size to

the zeolite pores are used, SiO_2 formation may occur on the acid sites located on the cross sectional space within the crystals, leading to modification of the acidity [30].

In this study, tri-phenyl silane (TPS) and phenyl silane (PS) were newly used as deactivators. The objectives of this study are elaborate characterization of modified ZSM-5 zeolites using TPS and PS. And then, the catalytic performance of modified nano-scale ZSM-5 zeolites for ATO reaction was investigated. Types of Si-compounds used for acidity modification affected the product selectivity. Moreover, the PS-treated nano-scale ZSM-5 showed a high selectivity of light olefin as well as a stable activity during ATO reaction. The relationship between the acidity modification and the catalytic performance was discussed.

2. Experimental

2.1 Preparation of ZSM-5 zeolite

Nano-scale ZSM-5 zeolite was prepared via hydrothermal synthesis using a water/surfactant/organic solvent (emulsion method) [31, 32]. An aqueous solution containing the Si and Al source material was obtained by hydrolyzing each metal alkoxide in a dilute tetra-propyl-ammonium hydroxide (TPAOH)/water solution. The water solution (10 ml) thus obtained was added to the surfactant/organic solvent (70 ml, surfactant concentration of 0.5 mol/l). Poly-oxyethylene-(15)-oleylether and cyclohexane were employed as the surfactant and

organic solvent, respectively. The water/surfactant/organic solvent thus obtained was poured into a Teflon-sealed stainless steel bottle and heated to 423 K for 72 h. In order to obtain macro-scale ZSM-5 as comparative catalyst, hydrothermal synthesis was also carried out without the surfactant/organic solvent (conventional method). The precipitates thus obtained were washed with alcohol, dried at 373 K for 12 h, and calcined at 823 K for 3 h in an air stream. Physically adsorbed and/or ion-exchanged sodium ions on the zeolite surface were removed and exchanged with NH_4^+ by a conventional ion exchange technique with a 10% NH_4NO_3 aqueous solution. The powdered NH_4^+-zeolite described above was pelletized, crushed and sieved to yield samples ca. 0.3 mm in diameter, and then heated to 823 K to yield a H-ZSM-5 zeolite for the ATO reaction.

2.2 Acidity control of ZSM-5 zeolite

The ZSM-5 zeolites were exposed to an organic silane compound vapor at 373 K in a nitrogen stream for 2 h, and the feed of the organic silane compound was then stopped to remove the physically adsorbed silane compounds on the zeolite surface. The sample was heated to 873 K to decompose the silane compound molecules chemically adsorbed on the acid sites and to leave silicon-containing carbonaceous residue on the acid sites. The sample was then calcined in an air stream at 873 K, where the silicon-containing carbonaceous residue was

converted into an SiO_2 unit on each acid site, resulting in deactivation of the acid sites. In other words, the SiO_2 units were formed on the acid sites where the silane compounds were chemically adsorbed. In our previous paper, we showed that SiO_2 units could be formed on the acid sites of the zeolite by the CCS method, and that the regioselective deactivation of the acid sites was achieved using silane compounds with different molecular sizes [28-30]. In this study, two kinds of silane compounds were newly employed; tri-phenyl silane (TPS) and phenyl silane (PS). The order of the molecular sizes of the silane compounds and the pore size of the MFI-type zeolite is: TPS > pore diameter of MFI ≈ PS. In the TPS treatment, because the molecular size of TPS is larger than the pore size of ZSM-5 zeolite, the acid sites on the outer surface can be selectively deactivated. In contrast, in the PS treatment, it is expected that the SiO_2 units are formed on acid sites located on the internal surface as well as outer surface of the crystal, leading to a decrease in acidic strength of the zeolite.

2.3 Characterization

The morphology and crystallinity of the obtained samples were analyzed using field emission scanning electron microscopy (FE-SEM; JSM-6500F, JEOL Co. Ltd.) and X-ray diffraction (XRD; JDX-8020, JEOL Co. Ltd.), respectively. The surface areas of the obtained samples were calculated by the BET-methods, using an N_2 adsorption isotherm (Belsorp mini,

BEL JAPAN Co. Ltd.). The Si/Al ratios of the obtained samples were evaluated by X-ray fluorescence measurements (XRF; Supermini, Rigaku Co. Ltd.). The acidity of the obtained samples was evaluated by the *ac*-NH_3-TPD method [33]. In the TPD experiment, the carrier gas was 1.0 % NH_3 (balance He), the heating rate was 5 K min^{-1}, and the temperature range was 373 to 823 K. The desorption of NH_3 molecules from the acid sites of the zeolite was measured under a 1.0 % NH_3-He atmosphere so that the TPD profile could be measured under complete adsorption equilibrium conditions, referred to as the *ac*-NH_3-TPD method. Pyridine adsorption on the obtained samples was observed by diffuse reflectance infrared Fourier transform (DRIFT) spectrometer equipped with a mercury cadmium telluride (MCT) detector (FT/IR-4100, JASCO Co. Ltd.). A total of 200 scans were averaged for each spectrum. Pre-treatment was conducted in vacuo at 723 K for 12h. And then, pyridine was introduced and adsorbed onto sample at 373 K for 2h, followed by the physically-adsorbed pyridine was removed in flowing N_2 at 373 K for 0.5 h, and remaining species were measured by FT-IR at 373K.

2.4 Cumene and TIPB cracking

In order to evaluate regioselective deactivation of acid sites, the catalytic cracking of isopropyl benzene (cumene) and 1,3,5-triisopropyl benzene (TIPB) was carried out using a

fixed-bed reactor under at a reaction temperature of 573 K N_2 flow at atmospheric pressure [34, 35]. The *W/F* ratio (*W*: amount of catalyst /g, *F*: feed rate /g h^{-1}) and the feed rate of cumene and TIPB was 0.13 h and 0.18 h, 1.0 ml/h and 1.33 ml/h, respectively. The catalyst weight was 0.15 g. The composition of the exit gas was measured by on-line gas chromatography (GC-2014, Shimadzu Co. Ltd.) with a Unipak-S column for the FID detector.

2.4 ATO reaction

The ATO reaction over ZSM-5 zeolite catalysts was carried out using a fixed-bed reactor at a reaction temperature of 723 K under N_2 flow at atmospheric pressure. The *W/F* ratio was 0.5 h. The feed rate of the acetone and the catalyst weight was 1.8 ml/h and 0.71 g, respectively. The composition of the exit gas was measured by on-line gas chromatography (GC-8A, Shimadzu Co. Ltd.) with a Porapak-Q column for the FID detector. The amount of coke deposited on the catalyst after the reaction was measured by thermogravimetric analysis (TG; TGA-50, Shimadzu Co. Ltd.).

3. Results and discussion

3.1 Preparation of ZSM-5 zeolites with different crystal sizes

Figure 1 shows X-ray diffraction patterns of the samples obtained by conventional hydrothermal and emulsion methods. The patterns of the samples showed peaks corresponding to the MFI-type zeolite. Figures 2 and 3 show FE-SEM micrographs and NH_3-TPD profiles of the obtained samples, respectively. As shown in Figure 2, the crystal size of the macro- and nano-ZSM-5 was approximately 1500 nm and 150 nm, respectively. Moreover, as shown in Figure 3, the ZSM-5 zeolites exhibited almost the same strong acidity regardless of the crystal size. Table 1 shows the Si/Al ratios measured by XRF and the surface area of the obtained samples. The Si/Al ratios were almost the same as the Si/Al ratio calculated from the Si and Al concentrations in the synthetic solution. Moreover, the nano-ZSM-5 exhibited almost the same BET surface area of 400 m^2/g as the macro-ZSM-5. In order to investigate the effects of crystal size and regioselective deactivation of the ZSM-5 zeolites on catalytic performance, these zeolites were used as catalysts for ATO reaction.

3.2 Characterization of ZSM-5 zeolites with different acid site locations

Although the nano-ZSM-5 is effective in the stabilization of catalytic activity, the catalyst lifetime is not sufficient, and product selectivity is unstable [21]. This resulted from coke formation on external surface of the zeolite crystal and non-volatile carbonaceous compound formation on pore surface within the crystal. These compounds inhibit diffusion and

adsorption of a reactant within the zeolite crystal. In order to overcome these problems, Suppression of the coke formation due to an excessive reaction of reactant/product is indispensable, and for this purpose, a regioselective deactivation of acid sites located on the external surface of the zeolite crystal is examined. One promising approach for this is the CCS (Catalytic Cracking of Silane) method, which can achieve control and/or modification of acidity of zeolite by regioselective formation of the SiO_2 unit [28-30]. In this study, two kinds of silane compounds were employed in the CCS method; Tri-phenyl silane (TPS) and phenyl silane (PS).

The FT-IR spectra of adsorbed pyridine and *ac*-NH_3-TPD profiles of the nano-ZSM-5 before/after CCS treatment can be seen in Figures 4 and 5, respectively. As shown in Fig. 4, Bands at around 1450 and 1540 cm^{-1} are attributed to Lewis acid sites (LAS) and Brønsted acid sites (BAS), respectively [36]. Although the IR absorbance was qualitatively measured, the intensity of the absorbance corresponding to the acid sites decreased after the CCS treatment, indicating that the acidity of the zeolite was weakened. There changes in the acidity due to the CCS treatment could be clearly observed from the NH_3-TPD profiles as shown in Figure 5. In both silane compounds, the amount of NH_3 desorbed from acid sites (mainly BAS) decreased after CCS treatment due to the formation of SiO_2 units on the acid sites. Moreover the TPD profiles showed that the amount of acid sites of the PS-treated nano-ZSM-5 was less than that of the TPS-treated nano-ZSM-5. The decrease in the amount of strong acid sites was attributed to

the relationship between the pore diameter of the ZSM-5 and the molecular size of the silane compound. In the case of TPS, because the molecular size of TPS is larger than the pore diameter of the ZSM-5, the acid sites located on the external surface were selectively deactivated. In contrast, because the molecular size of PS is slightly smaller than the pore diameter of the ZSM-5, not only acid sites on the external surface but also the acid sites on the internal surface were weakened. The difference in the molecular sizes in these silane compounds affected the number of deactivated acid site, leading to the difference in the NH_3-TPD profiles.

In CCS treatment, because the SiO_2 units are selectively formed on the acid sites, zeolitic pore properties such as the pore size and the surface area expected to be nearly-unchanged before and after treatment. In order to confirm this, the N_2 adsorption and cracking activity for alkyl-aromatics of nano-ZSM-5 zeolites before/after CCS treatment were examined. Figure 6 shows the N_2 adsorption isotherm of nano-ZSM-5 zeolites before/after CCS treatment. These modified zeolites exhibited almost the same micropore volume as compared with untreated nano-ZSM-5 zeolite. As mentioned above, CCS method has an insignificant effect on the pore properties of zeolite catalysts.

Figure 7 shows the results of cumene and TIPB cracking for nano-ZSM-5 before/after CCS treatment. The untreated nano-ZSM-5 (Figure 7(a)) has high catalytic activity for both

reactions. In this case, the conversion of TIPB gradually decreased with time on stream, indicating that the external acid sites became poisoned by coke formed on there [34, 35].

The CCS-treated nano-ZSM-5 (Figure 7(b) and 7(c)) showed almost no TIPB conversion, despite having some intact acid sites, as confirmed by the high cumene conversion comparable to untreated ZSM-5. A slight cracking of TIPB at initial reaction time may be due to the very small number of acid sites remaining on the external surface. No conversion of TIPB was observed after the initial reaction time, which means that the complete deactivation of the external acid site was readily accomplished by poisoning of the few residual acid sites on the external surfaces by a slight coke deposition during TIPB cracking at initial reaction time. These results strongly imply that acid sites on the external surface of nano-ZSM-5 are selectively deactivated after CCS treatment. In contrast, the ZSM-5 zeolites after CCS treatment exhibited an activity for cumene cracking as high as the untreated nano-ZSM-5. Because the minimum molecular diameter of cumene corresponding to benzene ring is almost the same as pore diameter of ZSM-5 zeolite, it is believed that the pore size of ZSM-5 zeolites is almost unchanged after CCS treatment, and the cumene can be diffuse in zeolitic channels of CCS-treated ZSM-5 zeolites. The initial cumene conversion in the PS-treated nano-ZSM-5 (51 C-mol%) was slightly lower than that in the TPS-treated nano-ZSM-5 (55 C-mol%), indicating that the SiO_2 units are formed on acid sites located on the internal surface as well as outer

surface of the crystal, whereas a sufficient acidity remained on the internal surface after PS treatment. In order to investigate the effects of the CCS treatment on catalytic performance, these modified nano-ZSM-5 were used as catalysts for ATO reaction.

3.3 Catalytic performance of ZSM-5 zeolites with different acid site locations

In the ATO reaction, isobutylene was first produced from aldol condensation products of acetone, followed by production of propylene, ethylene and aromatics over the acid sites. These light olefins are intermediate chemicals in the series of reactions with aromatics and coke as terminal products. The product selectivities and acetone conversion at initial reaction time over nano-ZSM-5 before/after CCS treatment are shown in Figure 8. The experimental result in nano-ZSM-5 was also shown in this figure for comparison. The CCS treatment to the nano-zeolite improved the light olefin selectivity (TPS : 57 C-mol%, PS : 58 C-mol%) and suppressed aromatics formation (TPS : 26 C-mol%, PS : 11 C-mol%) as compared with nano-ZSM-5 before CCS treatment (light olefins : 52 C-mol%, aromatics : 29 C-mol%). The improvement in the light olefins selectivities was ascribed to the suppression of non-selective and excessive reactions producing aromatics. After TPS-treatment, high ethylene and propylene yields were obtained. This is because the isobutylene produced reacted with each other to produce ethylene and propylene via dimerization/cracking of isobutylene over the acid sites

inside the zeolite crystal, where strong acidity remained after the TPS-treatment shown in Fig. 4. In contrast, in the PS treatment, high isobutylene yield as well as significantly low aromatic selectivity was achieved. After the PS treatment, the acid sites in cross sectional spaces inside the zeolite crystal, which are wide open spaces, were also deactivated besides the acid sites on the external surface. Accordingly, it is considered that SiO_2 unit formation on the external surface as well as intracrystalline pore surfaces caused suppression of the dimerization and cyclization of isobutylene followed by aromatics and coke formation. As a result, the CCS-treated nano-ZSM-5 was effective catalysts in the production of light olefins at high yield. Moreover, the regioselective deactivation of the acid sites was achieved by the CCS method with silane compounds with different molecular sizes, leading to the control of zeolite acidities and product selectivities.

Figure 9 shows the changes in acetone conversion with time on stream over ZSM-5 zeolites before/after PS treatment. Although the untreated nano-ZSM-5 showed stable activity as compared with the macro-ZSM-5, the conversion decreased to 20 C-mol% after 20 h. In contrast, the PS-treated nano-ZSM-5 maintained a high conversion above 70 % for 180 h. This result indicates excellent stability compared to the ZSM-5 before PS treatment. The amount of coke formed on the catalyst as measured by TG is listed in Table 2. Although the reaction time of the nano-ZSM-5 after CCS treatment using PS was much longer than that of the nano-ZSM-5

before the CCS treatment, the amount of coke formed on the PS-treated nano-ZSM-5 after the reaction (9.0 wt% after 180 h) was comparable to that of the macro- and nano-ZSM-5 before CCS treatment (macro-ZSM-5; 8.5 wt% after 6.5 h, nano-ZSM-5; 8.2 wt% after 30 h). Thus, the CCS treatment caused suppression of coke formation, leading to excellent stability. Figure 10 shows the product yields over PS-treated nano-ZSM-5. It is apparent that high light olefins yield (especially, isobutylene) was maintained for long reaction time (180 h), and this catalyst exhibited remarkable catalytic performance compared to our previous study [21, 22]. From these results, it is concluded that the regioselective deactivation for nano-ZSM-5 zeolite using CCS method was effective in improving the isobutylene yield and catalytic stability for the ATO reaction.

Conclusion

The regioselective deactivation of the acid sites was achieved by the CCS method with silane compounds with different molecular sizes, leading to the control of zeolite acidities. These modified nano-ZSM-5 zeolites were applied for ATO reaction, and the regioselective deactivation of acid sites by the CCS method caused the remarkable catalytic performance. Especially, the PS-treated nano-ZSM-5 zeolite was exhibited high light olefins yield with excellent stable activity as compared with macro- and nano-ZSM-5 before CCS treatment.

Acknowledgement

This work was supported by a Research Grant Program of the New Energy and Industrial Technology Development Organization (NEDO) of Japan and the Global COE Program (Project No. B01: Catalysis as the Basis for Innovation in Materials Science) from the Ministry of Education, Culture, Sports, Science and Technology, Japan.

References

[1] Y. Yoshimura, N. Kijima, T. Hayakawa, K. Murata, K. Suzuki, F. Mizukami, K. Matano, T. Konishi, T. Oikawa, M. Saito, T. Shiojima, K. Shiozawa, K. Wakui, G. Sawada, K. Sato, S. Matsuo, N. Yamaoka, *Catal. Surv. Jpn.,* **4** (2000)157-167

[2] O. Bortnovsky, P. Sazama, B. Wichterlova, *Appl. Catal. A Gen.,* **287** (2005) 203-213

[3] C. Mei, P. Wen, Z. Liu, Y. Wang, W. Yang, Z. Xie, W. Hua, Z. Gao, *J. Catal.,* **258** (2008) 243-249

[4] A. Corma, J. Planelles, J. Sanchezmarin, F. Tomas, *J. Catal.,* **93** (1985) 30-37

[5] S.M. Babitz, B.A. Williams, J.T. Miller, R.Q. Snurr, W.O. Haag, H.H. Kung, *Appl. Catal. A Gen.,* **179** (1999) 71-86

[6] H. Mochizuki, T. Yokoi, H. Imai, R. Watanabe, S. Namba, J. N. Kondo, T. Tatsumi,

Micropor. Mesopor. Mater., **145** (2011)165-171

[7] K. Kubo, H. Iida, S. Namba, A. Igarashi, *Micropor. Mesopor. Mater.,* **149** (2012)126-133

[8] S. Inagaki, S. Shinada, Y. Kaneko, K. Takechi, R. Komatsu, Y. Tsuboi, H. Yamazaki, J.N. Kondo, Y. Kubota, *ACS Catal.,* **3** (2013) 74-78

[9] H. Konno, T. Okamura, Y. Nakasaka, T. Tago, T. Masuda, *J. Jpn. Petrol. Inst.*, **55** (2012) 267-274

[10] H. Konno, T. Okamura, Y. Nakasaka, T. Tago, T. Masuda, *Chem. Eng. J.,* **207-208** (2012) 460-467

[11] H. Konno, T. Tago, Y. Nakasaka, R. Ohnaka, J. Nishimura, T. Masuda, *Micropor. Mesopor. Mater.,* **175** (2013) 25-33

[12] M. stocker, *Micropor. Mesopor. Mater.,* **29** (1999) 3-48

[13] F. J. Keil, *Micropor. Mesopor. Mater.,* **29** (1999) 49-66

[14] Y. Kumita, J. Gascon, E. Stavitski, J.A. Moulijn, F. Kapteijn, *Appl. Catal. A Gen.,* **391** (2011) 234-243

[15] T. Meng, D. Mao, Q. Guo, G. Lu, *Catal. Comm.,* 21 (2012) 52-57

[16] Y. Furumoto, Y. Harada, N. Tsunoji, A. Takahashi, T. Fujitani, Y. Ide, M. Sadakane, T. Sano, *Appl. Catal. A Gen.,* **399** (2011) 262-267

[17] D. Goto, Y. Harada, Y. Furumoto, A. Takahashi, T. Fujitani, Y. Oumi, M. Sadakane, T. Sano, *Appl. Catal. A Gen.,* **383** (2010) 89-95

[18] C. Yu, Q. Ge, H. Xu, W. Li, *Appl. Catal. A Gen.,* **315** (2006) 58-67

[19] L. Liu, Q. Deng, Y. Liu, T. Ren, Z. Yuan, *Catal. Comm.,* **16** (2011) 81-85

[20] R.J. Schmidt, *Appl. Catal. A Gen.,* **280** (2005) 89-103

[21] T. Tago, H. Konno, M. Sakamoto, Y. Nakasaka, T. Masuda, *Appl. Catal. A Gen,* **403** (2011) 183-191

[22] T. Tago, H. Konno, S. Ikeda, S. Yamazaki, W. Ninomiya, Y. Nakasaka, T. Masuda, *Catal. Today,* **164** (2011) 158-162

[23] S.H. McAllister, W.A. Bailey, C.M. Bouton, *J. Am. Chem. Soc.,* **62** (1940) 3210-3215

[24] J. Cejka, L. Kubelkova, P. Jiru, *Collect. Czech. Chem. Commun.,* 54 (1989) 2054-2062

[25] J. Cejka, P. Jiru, *Collect. Czech. Chem. Commun.,* 54 (1989) 2998-3002

[26] L. Kubelkova, J. Cejka, J. Novakova, *Zeolite* **11** (1991) 48-53

[27] A.G. Panov, J.J. Fripiat, *J. Catal.,* **178** (1998) 188-197

[28] T. Tago, K. Iwakai, K. Morita, K. Tanaka, T. Masuda , *Catal. Today,* **105** (2005) 662-666

[29] T. Tago, M. Sakamoto, K. Iwakai, H. Nishihara, S. R. Mukai, T. Tanaka, T. Masuda, , *J. Chem. Eng. Jpn*., **42** (2009) 162-167

[30] T. Masuda, N. Fukumoto, M. Kitamura, S.R. Mukai, K. Hashimoto, T. Tanaka, T. Funabiki,

Micropor. Mesopor. Mater. **48** (2001)239-245

[31] T. Tago, M. Nishi, Y. Kouno, T. Masuda, *Chem. Lett.,* **33** (2004) 1040-1041

[32] T. Tago, H. Konno, Y. Nakasaka, T. Masuda, *Catal. Surv. Asia*, **16** (2012) 148-163

[33] T. Masuda, Y. Fujikata, S. R. Mukai, K. Hashimoto, *Appl. Catal. A Gen.,* **165** (1997) 57-72

[34] C. Anand, I. Toyama, H. Tamada, S. Tawada, S. Noda, K. Komura, Y. Kubota, S.W. Lee, S.J. Cho, J.H. Kim, G. Seo, A. Vinu, Y. Sugi, *Ind. Eng. Chem. Res.,* **51** (2012) 12214–12221

[35] S. Inagaki, S. Shinoda, Y. Kaneko, K. Takechi, R. Komatsu, Y. Tsuboi, H. Yamazaki, J.N. Kondo, Y. Kubota, *ACS Catal.,* **3** (2013) 74-78

[36] E.P. Parry, *J. Catal.,* **2** (1963) 371-379

Figure and Table captions

Figure 1. XRD patterns of (a) macro- and (b) nano-ZSM-5 zeolites

Figure 2. SEM micrographs of (a) macro- and (b) nano-ZSM-5 zeolites

Figure 3. NH_3-TPD profiles of macro- and nano-ZSM-5 zeolites

Figure 4. NH_3-TPD profiles of the nano-ZSM-5 zeolites before/after CCS treatment

Figure 5. FT-IR spectra of pyridine-adsorbed nano-ZSM-5 zeolites. (a) before CCS treatment, (b) After TPS treatment and (c) After PS treatment

Figure 6. N_2 adsorption isotherm of nano-ZSM-5 zeolites before/after CCS treatment

Figure 7. The results of catalytic cracking of isopropyl benzene (cumene) or 1,3,5-triisopropyl benzene (TIPB) over (a) untreated nano-ZSM-5, (b) PS-treated nano-ZSM-5 and (c) TPS-treated nano-ZSM-5 zeolites

Figure 8. Product selectivities for reaction over nano-ZSM-5 before/after CCS treatment at initial reaction time (2.5h)

Figure 9. Changes in acetone conversion with time on stream over macro- and nano-ZSM-5 before/after PS treatment

Figure 10. Product yields with time on stream over PS-treated nano-ZSM-5 zeolite

Table 1. BET and external surface areas of macro- and nano-ZSM-5 zeolites. S_{BET}: surface area by BET method, S_{ext}: external surface area by *t*-method

Table 2. Coke amount of ZSM-5 zeolite catalysts after the reaction measured by TG

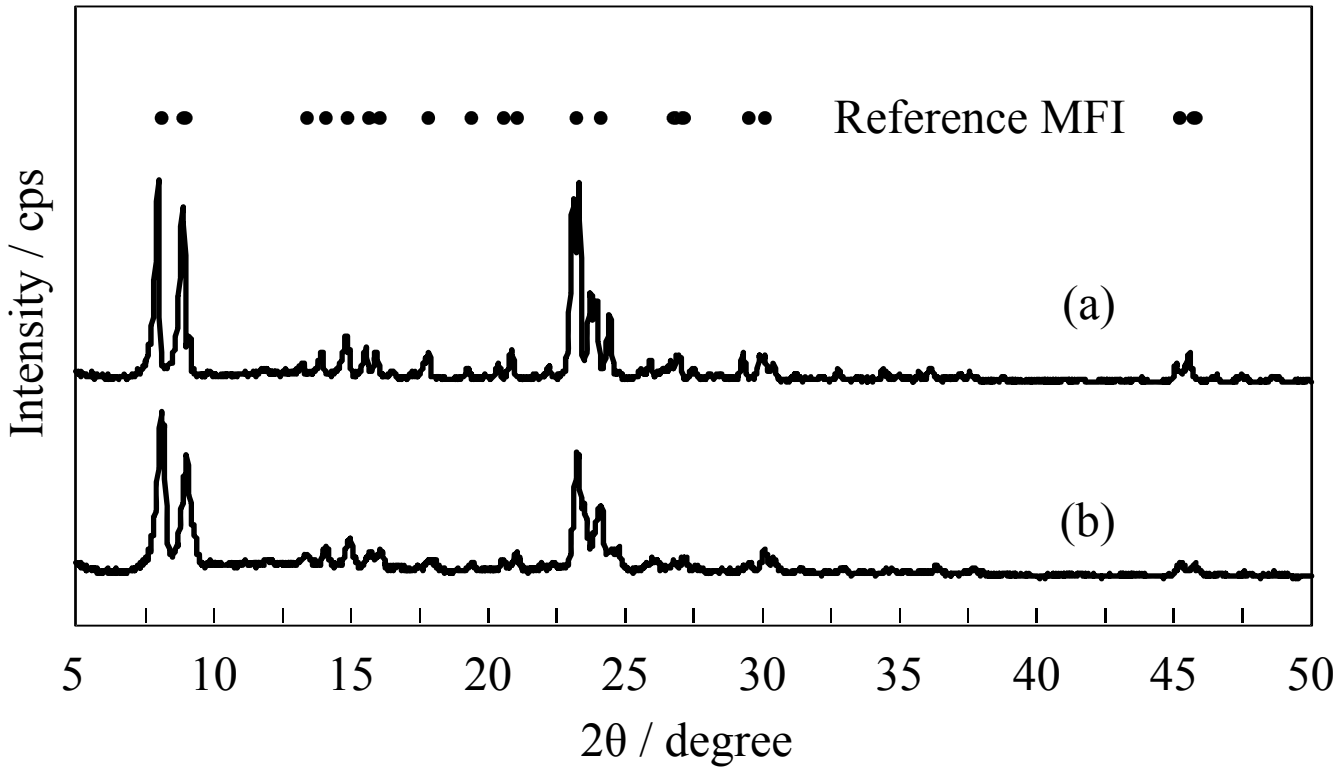

Figure 1. XRD patterns of (a) macro- and (b) nano-ZSM-5 zeolites

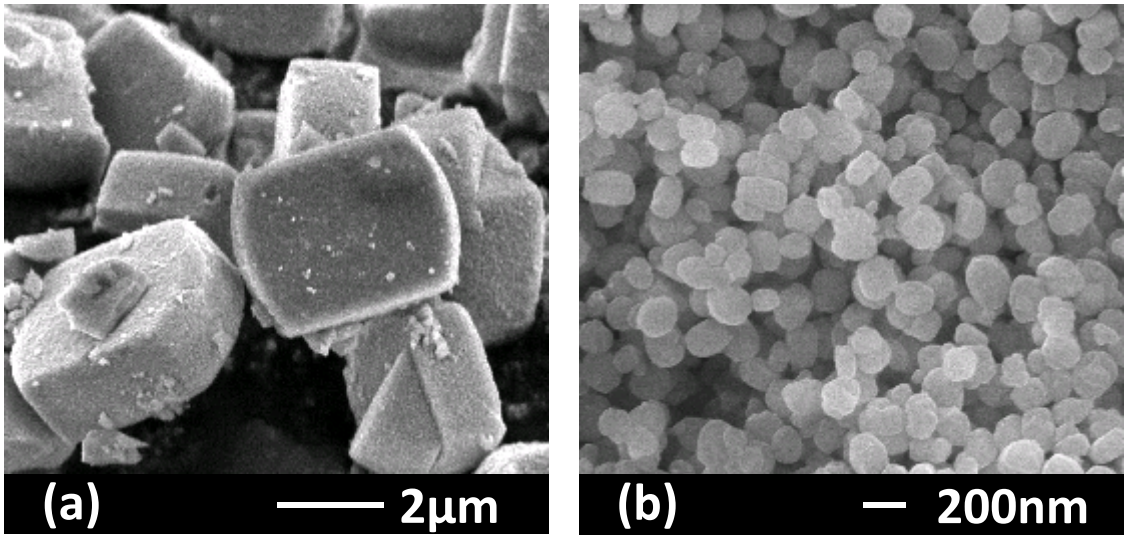

Figure 2. SEM micrographs of (a) macro- and (b) nano-ZSM-5 zeolites

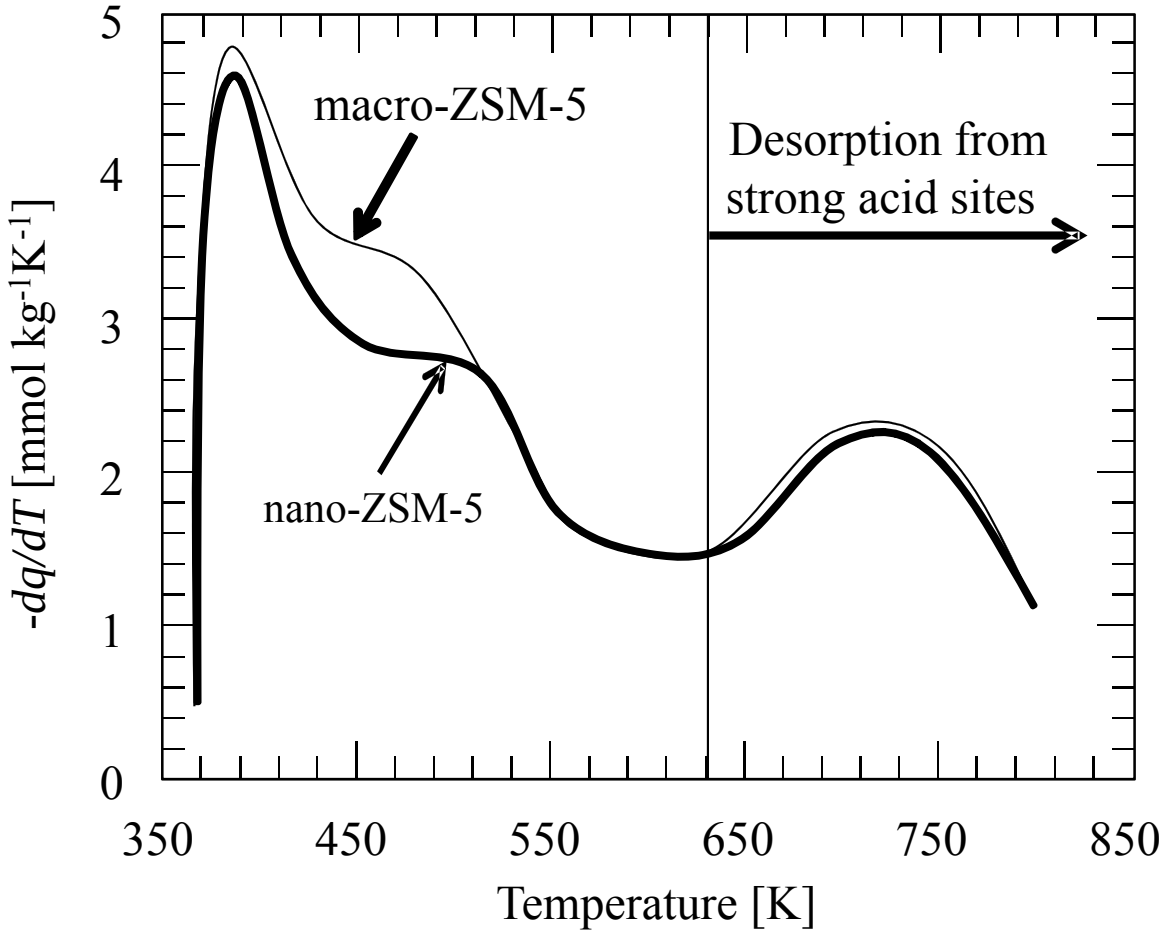

Figure 3. NH_3-TPD profiles of macro- and nano-ZSM-5 zeolites

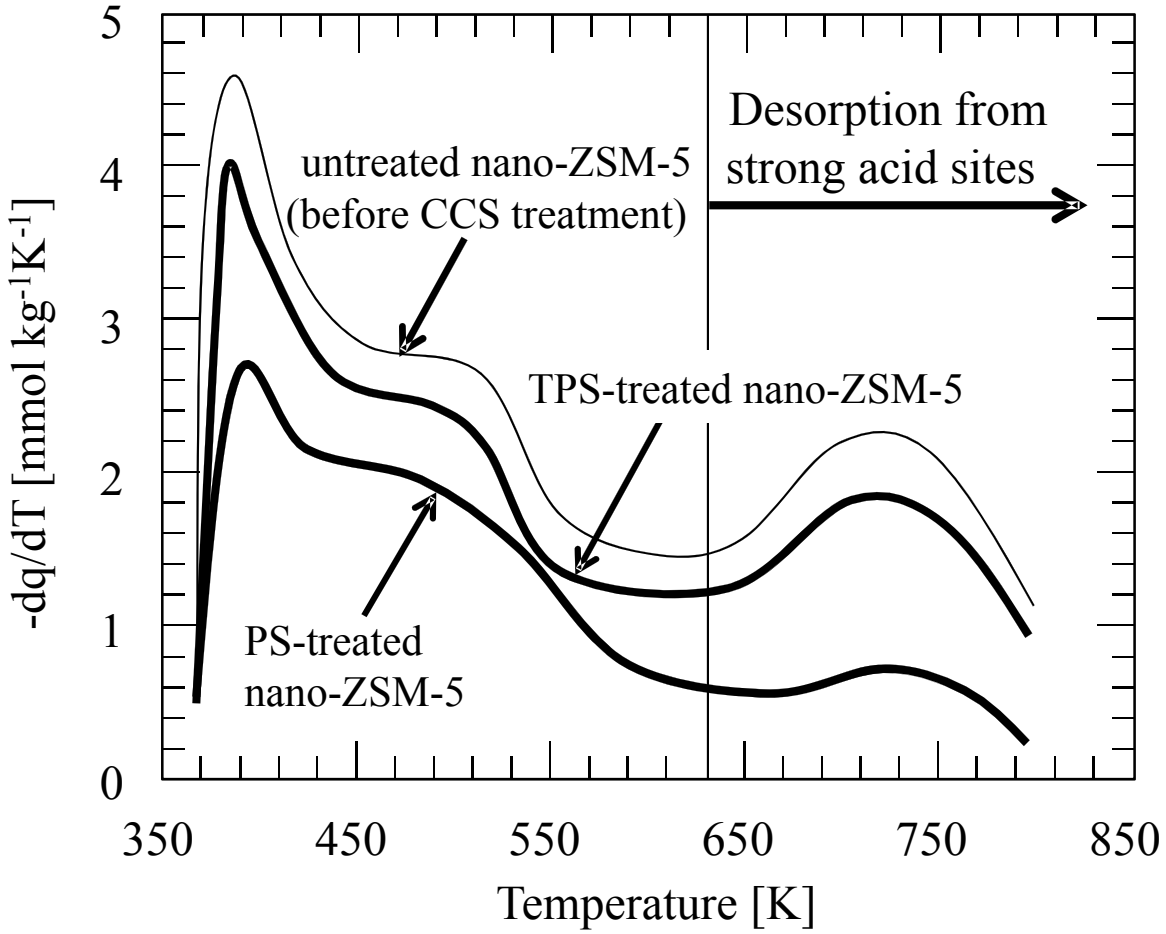

Figure 4. NH_3-TPD profiles of the nano-ZSM-5 zeolites before/after CCS treatment

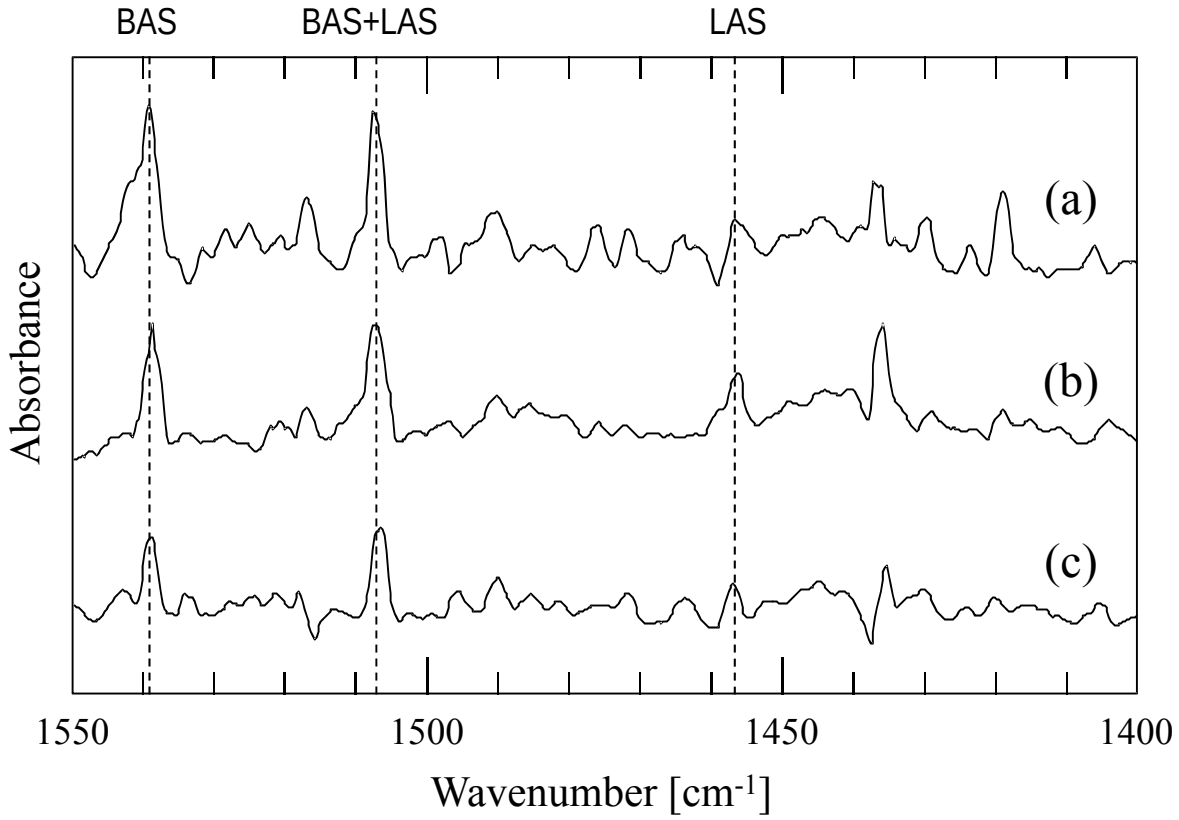

Figure 5. FT-IR spectra of pyridine-adsorbed nano-ZSM-5 zeolites.
(a) before CCS treatment, (b) After TPS treatment and (c) After PS treatment

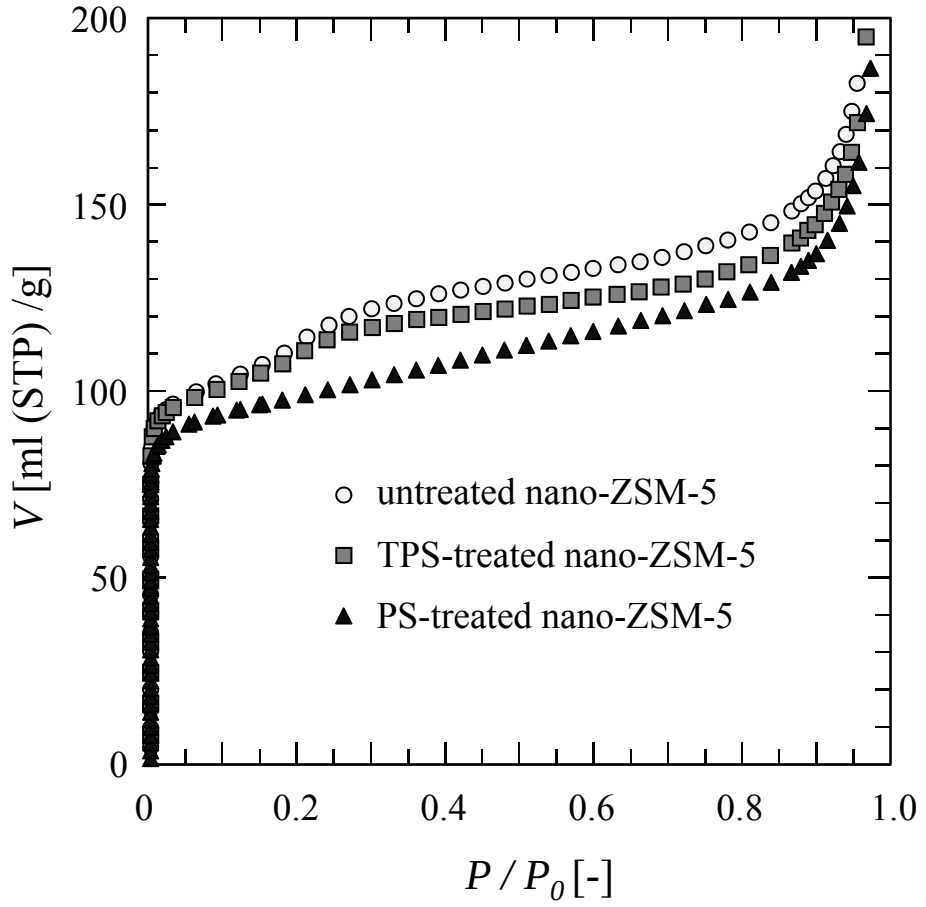

Figure 6. N_2 adsorption isotherm of nano-ZSM-5 zeolites before/after CCS treatment

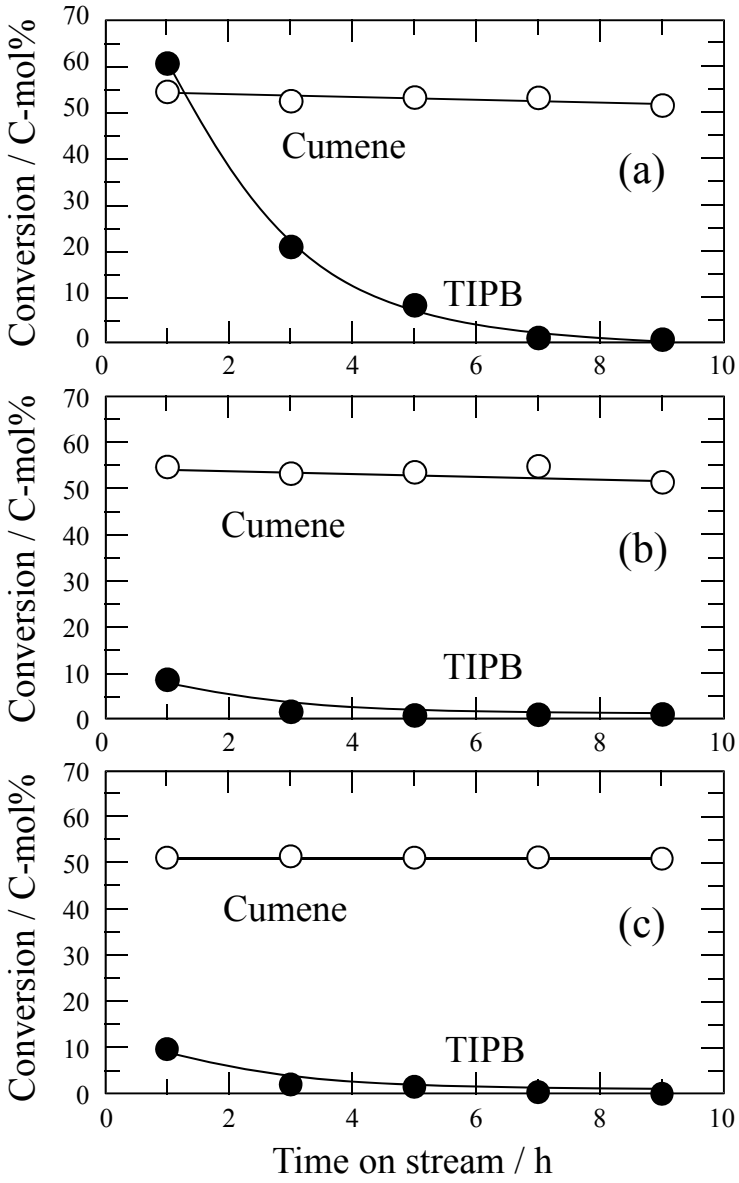

Figure 7. The results of catalytic cracking of isopropyl benzene (cumene) or 1,3,5-triisopropyl benzene (TIPB) over (a) untreated nano-ZSM-5, (b) PS-treated nano-ZSM-5 and (c) TPS-treated nano-ZSM-5 zeolites

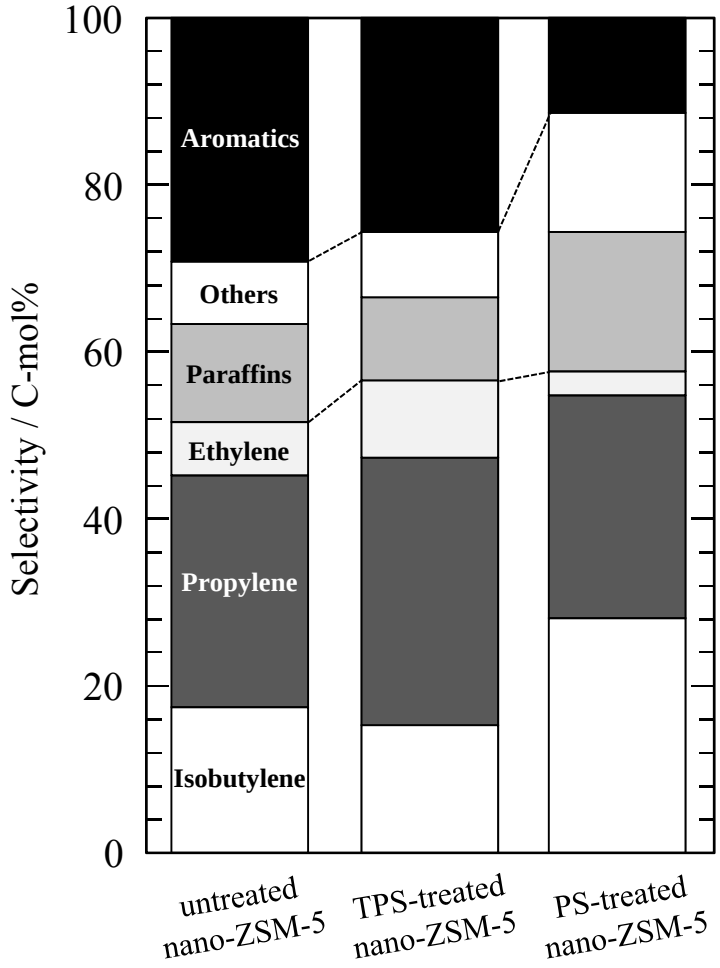

Figure 8. Product selectivities for reaction over nano-ZSM-5 before/after CCS treatment at initial reaction time (2.5h)

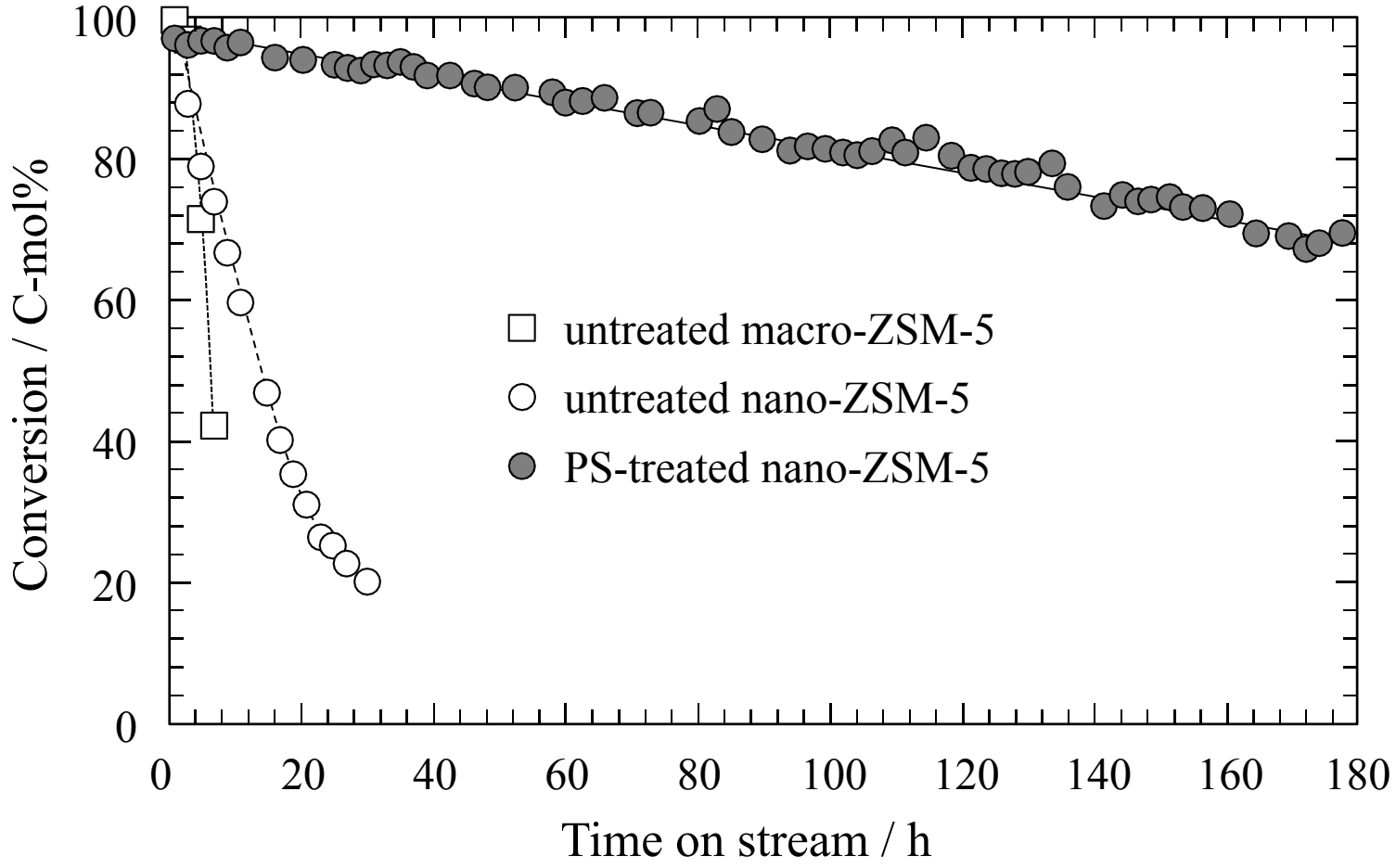

Figure 9. Changes in acetone conversion with time on stream over macro- and nano-ZSM-5 before/after PS treatment

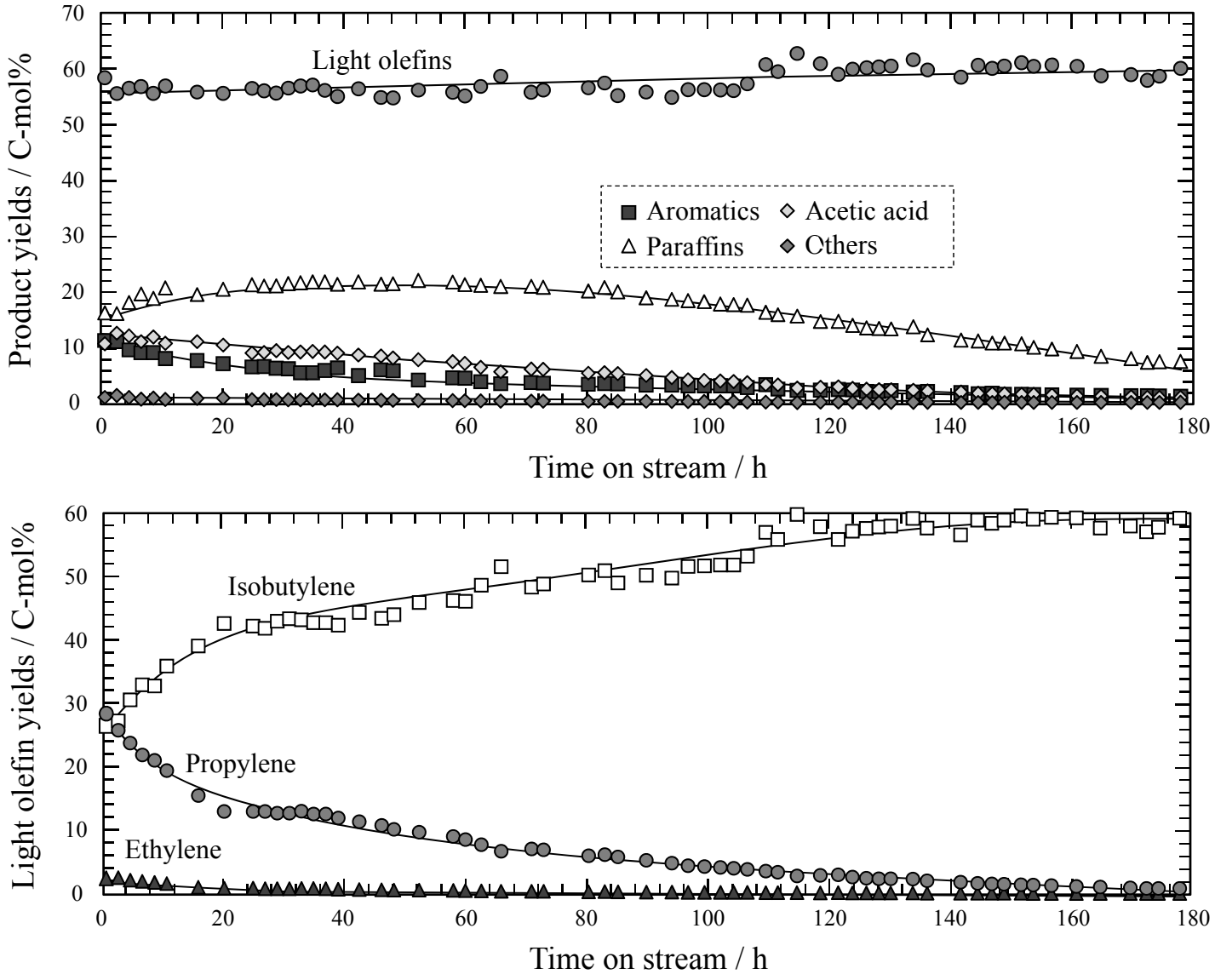

Figure 10. Product yields with time on stream over PS-treated nano-ZSM-5 zeolite

Zeolite	S_{BET} (m^2g^{-1})	Si/Al $_{measured\ by\ XRF}$
untreated macro-ZSM-5	405	81
untreated nano-ZSM-5	400	89
TPS-treated nano-ZSM-5	391	-
PS-treated nano-ZSM-5	370	-

Table 1. The surface areas by BET-method and Si/Al ratios of macro- and nano-ZSM-5 zeolites.

Zeolite	Reaction time [h]	Coke amount [wt%]
untreated macro-ZSM-5	6.5	8.5
untreated nano-ZSM-5	30.0	8.2
PS-treated nano-ZSM-5	180.0	9.0

Table 2. Coke amount of ZSM-5 zeolite catalysts after the reaction measured by TG